Tuijin Jishu/Journal of Propulsion Technology
ISSN: 1001-4055
Vol. 44 No. 6 (2023)

Thermal Radiation on Three Dimensonal Casson nanofluid Flow with Convective Boundary Layer Via Stretching Sheet

Motamari Madhu[1*, 2*], Maddileti Pasupula[3]

[1*] *Department of Mathematics, University College, Palamuru University, Mahabubnagar-509001, Telangana, India*

[2*, 3]*Departement of Mathematics, University College of Science and Informatics, Mahatma Gandhi Universitu, Nalgonda-508254, Telangana, India*

* *Corresponding Author:*

Abstract: - The numerical analysis related to the behavior of Casson nanofluid (NFs) in a three-dimensional boundary layer (BL) motion via stretching sheet (SS). The study focuses on analyzing the behavior of a Casson nanofluid, which is a type of non-Newtonian fluid, in a three-dimensional boundary layer with heat and mass transfer. The BL is formed via stretching sheet, which is a common configuration in fluid dynamics. The main goal of this research is to understand how Casson liquid behaves in this specific scenario, with a particular emphasis on heat and mass transfer. Understanding this behavior has practical applications in various industries, including chemical manufacturing, thermoelectric sciences, biomedical devices, polymer extrusion, and thermal system enhancement. The study appears to involve solving partial differential equations (PDEs) related to fluid flow, heat transfer, and mass transfer. These PDEs are transformed into ordinary differential equations (ODEs) using standard similarity variables. To solve the ODEs, the researchers employ the Runge-Kutta-Fehlberg (R-K-F) IV order iterative scheme. It appears that higher values of the Biot number and thermal radiation can significantly affect the temperature and concentration profiles in the Casson liquid flow.

Keywords*: Thermal Radiation, Casson Fluid, Nanofluid, Stretching Sheet.*

1. Introduction

In recent times, there has been a notable surge in interest surrounding the exploration of nanofluids within the domains of fluid dynamics and heat transfer. It has emphasized sustainability through its focus on multiple nanofluid compositions, novel manufacturing approaches, and their roles in renewable energy. The term Nanofluids was first devised by Choi et al. [1] explained distinct class of precisely tailored heat transfer fluids. These fluids include metallic particles with an average size of around 10 nanometers which can be created utilizing modern nanophase technologies. Masuda et al. [2] ferreted out how the base solution's thermal conductivity would be impacted through the distribution of infinitesimal amounts of ultrafine particles in a liquid, where water was used as the solvent in the research to successfully develop a stable dispersion system. Cheng [3] encountered on multifaceted nature of HT by natural convection in porous media via non-Newtonian liquid, especially in the backdrop of a vertical cone. The study additionally investigated the challenges that were brought forth by mixed thermal boundary conditions. Panduro et al. [4] utilized the use of leading-edge numerical methods, and generated groundbreaking and core findings that have significant consequences on this area of study. They are being researched specifically for use in parabolic-trough collectors operating between 100°C and 300°C. Despite its potential, challenges include maintaining stability, addressing environmental concerns, and growing results. Mostafizur et al. [5] examined on the increased HT performance of NFs, which are nanoparticle suspensions that surpass conventional HT liquid. The study investigates the thermophysical properties of NFs including Aluminium Oxide (Al2O3) NPs in methanol, as well as their thermal conductivity, viscosity, and density. Recently custom-designed electronic chips are becoming more common due to spatial limitations in applications. The use of NFs in heat pipes has gained attention for their exceptional HT performance which was explained by Rangasamy et al. [6].

Due to the diversity of non-Newtonian liquid and the variety of applications they cover, researchers often use different models to capture specific behaviours. The Casson fluid model is just one example of such models, and it is well-suited for describing materials with yield stress and shear-thinning properties. Researchers continue to develop and refine models to better represent the behaviour of non-Newtonian liquid in various scenarios, contributing to advancements in multiple industries. The Casson liquid model has found applications in various industries such as "petroleum sector, aerodynamics, paper manufacturing, food industry, pharmaceuticals". Saidulu and Venkata [7] Investigated the Keller box approach and studied the flow of Casson fluid via exponentially extending sheet. Khan et al. [8] explored entropy generation in the radiative spinning motion of Casson NFs. Zeeshan [9] evaluated various flow scenarios in applied sciences. Prabhakar Reddy et al. [10] used finite element methods to analyze the effects of diffusion-thermo and rotation on HT in Casson liquid. Goud Bejawada et al. [11] investigated the effects of TR, chemical reaction, and heat source on MHD Casson liquid motion via inclined SS within a Forchheimer porous medium. Riaz Khan et al. [12] studied radiated stagnation point motion of time-dependent Casson fluid. Jalili et al. [13] examined the effect of thermo-diffusion, electrical field, and NLTR. Bhagya Lakshmi et al. [14] investigated convective HMT in MHD motion of a Casson liquid via curved surface. Sivakumar et al. [15] observed that the rate of HT in Casson liquid increases with magnetic field intensity up to a certain threshold, beyond which it decreases.

Asifa et al. [16] investigated unsteady flow of a rate-type fluid near a vertical plate. Waqas et al. [17] investigated TR and heat source-sink effects on hybrid nanofluids. Yaseen et al. [18] explored heat transfer characteristics between plates. Tarakaramu et al. [19] examined heat transmission in Williamson NFs motion across a porous medium on a SS. Tarakaramu et al. [20] investigated HMT in a three-dimensional couple stress Casson liquid motion. Waqas et al. [21] examined three-dimensional particle movement near a SS. Tarakaramu et al. [22] studied heat transmission in a 3D environment under the influence of a magnetic field. Tarakaramu et al. [23] explored the interplay between activation energy and fluid dynamics in MHD NFs motion. Jagadeesh et al. [24] analyzed the detailed interplay between 3D NFs motion, thermal radiation, heat absorption, and convective HMT on a linearly SS. Bejawada and Nandeppanavar et al. [25] explored influence of TR on heat transfer characteristics of a micropolar liquid motion via vertical moving porous plate under MHD conditions. Vanitha et al. [26] investigated complex interactions involving MHD, Marangoni effect, nanoparticles, TR, and HT within a porous sheet. Miroshnichenko et al. [27] studied energy transfer rate in various structures with applications in building design and materials engineering.

Ghoneim and Megahed [28] used numerical analysis to unravel the complex behavior of non-Newtonian fluids flowing via SS, considering the impact of TR. Alrehili [29] contributed many engineering applications by investigating the behavior of dissipative Carreau NFs flowing via nonlinearly stretching sheets, considering the influence of TR. Rehman. [30] explored how TR and thermal conductivity mutually affect non-Newtonian fluids exhibiting multiple motion regimes. By deciphering the complex interactions for various practical applications.

2. Mathematical Analysis

The mathematical model as consider by using following aspects such as:

- Consider the 3D convective incompressible couple stress non-Newtonian Casson liquid motion via with thermal radiation.
- We considered the liquid motion through x^*, y^* directions.
- The fluid motion considers at stretching sheet in z^* is vanishes.
- The velocity components of axial and transverse direction $u_1 = U_w^*(x^*) = a_1 x^*,\ \ v_1 = V_w^*(x^*) = b_1 y^*$ as shown in **Fig.1**.

The rheological equation of Casson liquid motion has to be consider as follows

$$\tau_{ij} = \begin{cases} \left(2\mu_0^* + \dfrac{2p_y^*}{\sqrt{2\pi^*}}\right)e_{ij}, & if\ \pi^* \geq \pi_1^* \\ \left(2\mu_0^* + \dfrac{2p_y^*}{\sqrt{2\pi_1^*}}\right)e_{ij}, & if\ \pi^* < \pi_1^* \end{cases} \tag{1}$$

Where, $p_y^* = e_{ij}e_{ij}$ and $\beta = \mu_B^*\sqrt{2\pi_1^*}\,/\,\mathrm{p}_y^*$.

The fundamental equations of continuity, heat and concentration Eqs can be formulated by using eq. (1)

$$\frac{\partial u_1}{\partial x^*} + \frac{\partial v_1}{\partial y^*} + \frac{\partial w_1}{\partial z^*} = 0 \tag{2}$$

$$u_1\frac{\partial u_1}{\partial x^*} + v_1\frac{\partial u_1}{\partial y^*} + w_1\frac{\partial u_1}{\partial z^*} = \upsilon^*\left(1 + \frac{1}{\beta}\right)\frac{\partial^2 u_1}{\partial\left(z^*\right)^2} \tag{3}$$

$$u_1\frac{\partial v_1}{\partial x^*}+v\frac{\partial v_1}{\partial y^*}+w\frac{\partial v_1}{\partial z^*}=\upsilon^*\left(1+\frac{1}{\beta}\right)\frac{\partial^2 v_1}{\partial\left(z^*\right)^2}_1 \tag{4}$$

$$u_1\frac{\partial\Phi^*}{\partial x^*}+v_1\frac{\partial\Phi^*}{\partial y^*}+w_1\frac{\partial\Phi^*}{\partial z^*}=\alpha_1\frac{\partial^2\Phi}{\partial z^{*2}}+\tau_1\left(D_B\frac{\partial\Phi}{\partial z^*}\frac{\partial\psi}{\partial z^*}+\frac{D_\Phi}{\Phi_\infty}\left(\frac{\partial\Phi}{\partial z^*}\right)^2\right)-\frac{1}{(\rho c)_f}\frac{\partial q_r}{\partial z^*} \tag{5}$$

$$u_1\frac{\partial\psi}{\partial x^*}+v_1\frac{\partial\psi}{\partial y^*}+w_1\frac{\partial\psi}{\partial z^*}=\left(D_B\frac{\partial^2\psi}{\partial\left(z^*\right)^2}+\frac{D_T}{\Phi_\infty}\left(\frac{\partial^2\Phi}{\partial\left(z^*\right)^2}\right)\right) \tag{6}$$

The present relevant model boundary conditions as

$$\left.\begin{array}{l} z^*=0 \quad at \quad u_1=a_1x^* \quad v=b_1y^* \quad w_1=0, \ -k\dfrac{\partial T^*}{\partial z^*}=h_1(T_f^*-T^*) \quad -D^*\left(\dfrac{\partial C^*}{\partial z}\right)=h_2\left(C_f^*-C^*\right) \\ z^*\to\infty \quad as \quad u_1\to 0 \ \ v_1\to 0, \ u_1'\to 0, \ v_1'\to 0, \ T^*\to T_\infty^*, \ C^*\to C_\infty^* \end{array}\right. \tag{7}$$

The similarity transformations as below

$$\left.\begin{array}{l} \eta=\sqrt{\dfrac{a_1}{\upsilon_f^*}}z^*, \quad u_1=a_1x^*f'(\eta), \quad v_1=a_1y^*g'(\eta), \quad w_1=-\sqrt{a_1\upsilon^*}(f(\eta)+g(\eta)) \\ \qquad \theta(\eta)=\dfrac{\Phi-\Phi_\infty}{\Phi_w-\Phi_\infty}, \qquad \phi(\eta_1)=\dfrac{\psi-\psi_\infty}{\psi_w-\psi_\infty} \end{array}\right\} \tag{8}$$

Using above **Eq. (8)**, we are converting **Eq. (3)-(6)** into below format

$$f'''=\left[1\Big/\left(1+\beta/\beta\right)\right]\left[-f''(f+g)+2f'(f'+g')\right] \tag{9}$$

$$f'''=\left[1\Big/\left(1+\beta/\beta\right)\right]\left[-g''(f+g)+2g'(f'+g')\right] \tag{10}$$

$$\theta''=\left[1\Big/\left(3+4R/3\Pr R\right)\right]\left[-(f+g)\theta'-N_b\theta'\phi'-N_t(\theta')^2\right] \tag{11}$$

$$\phi''=-Le\left((f+g)\phi'-\left(N_t/N_b\right)\left[1\Big/\left(3+4R/3\Pr R\right)\right]\left[-(f+g)\theta'-N_b\theta'\phi'-N_t(\theta')^2\right]\right) \tag{12}$$

Corresponding B.Cs. as below

$$\left.\begin{array}{l} f=0, \quad g=0, \quad f'=1, \quad g'=1, \quad \theta'=-Bi_t(1-\theta), \quad \phi'=-Bi_c(1-\phi) \quad at \quad \eta=0 \\ f'\to 0, \quad g'\to 0, \quad \theta\to 0, \quad \phi\to 0, \qquad\qquad as \quad \eta\to\infty \end{array}\right\} \tag{13}$$

Moreover, the skin-friction coefficient and Nusselt number are below

$$\left.\begin{array}{l} \mathrm{Re}_x^{0.5}C_{fx}=(1+\dfrac{1}{\beta})f''(0), \quad \mathrm{Re}_x^{0.5}C_{fy}=(1+\dfrac{1}{\beta})g''(0) \\ \mathrm{Re}_x^{-0.5}Nu_x=-\theta'(0), \quad \mathrm{Re}_x^{-0.5}\mathrm{Sh}=-\phi'(0) \end{array}\right\} \tag{14}$$

3. Results and Discussion

Fig. 2 predicts the β (Casson Fluid Parameter) on $f'(\eta)$. These observations suggest that the Casson fluid parameter plays a critical role in determining both the velocity profile within the boundary layer. Increasing β results in reduced velocity. This finding is likely crucial for understanding the behaviour of non-Newtonian fluids in various applications and processes where boundary layers are involved.

Fig. 3 presented $\Pr$ (Prandtl number) on $\theta(\eta)$. This behaviour is consistent with the physical interpretation of the Prandtl number. A higher Prandtl number implies that heat is conducted less efficiently within the fluid compared to the momentum transfer (velocity). This can have significant implications for heat transfer processes, such as conduction, convection, and boundary layer phenomena. Physically, materials with higher Prandtl numbers are often less efficient at conducting heat and may experience slower changes in temperature profiles compared to materials with lower Prandtl numbers.

Fig. 4(a)-4(b) presented the N_b (Brownian Motion Parameter) on $\theta(\eta)$, $\phi(\eta)$. We have described characteristic of the influence of Brownian motion on nanoparticle dispersion and transport within a fluid. When N_b is higher, it implies that Brownian motion becomes more significant, causing nanoparticles to move more erratically within the fluid. This increased movement can lead to enhanced mixing and heat transfer, which, in turn, results in a thicker thermal boundary layer and higher temperatures within the nanofluid. Physically, the influence of parameter like N_b is essential in the design and optimization of nanofluid-based systems, where controlling temperature profiles and heat transfer efficiency are critical considerations.

In summary of N_t (Thermophoresis Parameter) exhibited on $\theta(\eta)$, $\phi(\eta)$ as shown in Figs. 4(a)-4(b), respectively. The rise in fluid temperature and concentration with an increase in the thermophoresis parameter N_t is linked to the behavior of nanoparticles within the fluid. Physically, the thermophoretic force induces nanoparticles near the hot boundary to migrate towards the cold fluid, which results in a thicker thermal boundary layer. This phenomenon is significant in understanding how nanoparticles disperse and impact temperature distributions within fluids, particularly in applications involving heat transfer and nanofluids.

The characteristics of thermal Biot Number on $\theta(\eta)$, $\phi(\eta)$ predicts in **Fig. 5-6**, respectively. It is observed that, indicative of the interplay between conduction and convection heat transfer and concentration. A high Biot number implies that convection heat transfer as well as concentration is enhancing, leading to a rapid increase in temperature and concentration near the boundary. This behavior can be seen in systems where the solid boundary is in direct contact with a fluid, and heat is transferred from the solid to the fluid through convection. Physically, the influence of the Biot number is crucial in applications involving heat exchangers, cooling of solid surfaces, and various other situations where heat transfer between a solid and a surrounding fluid is essential. High Biot numbers often indicate efficient convective heat transfer, while low Biot numbers suggest that conduction within the solid is dominant.

Fig. 7 shows characteristics of Lewis number on $\phi(\eta)$. These observations indicate that the Lewis number plays a significant role in determining the behavior of nanoparticle concentration profile in the presence of Brownian diffusion. A higher Lewis number implies that thermal diffusion is more dominant relative to molecular diffusion, leading to decreased Brownian diffusion and, consequently, a thinner concentration boundary layer and reduced nanoparticle concentration near the sheet. Physically, it has various applications involving nanofluids, such as in heat transfer, materials processing, and nanomaterial deposition, as it helps in predicting and controlling the distribution of nanoparticles in a fluid.

Fig. 8 exhibited the R on $\theta(\eta)$. A declined in the thermal radiation parameter can indeed result in less heat being transferred to a Casson fluid, which in turn leads to a low in temperature and thermal BL thickness. Thermal radiation is the transfer of heat in the form of electromagnetic waves, primarily in the infrared region of the electromagnetic spectrum. Physically, decreasing the TR parameter can be achieved by various means, such as increasing the temperature of the radiating surface or using materials that emit more thermal radiation. This can be important in engineering and heat transfer applications, where controlling or enhancing heat transfer processes is essential.

Table. 1 presented the variation of Casson Fluid Parameter on Skin friction coefficients and **Table 2** predicts the effect of Brownian motion and Thermophoresis parameter as well as Biot number for temperature and concentration Heat and Mass transfer rate:

4. Conclusion

The main contribution results as presented as following:

- The velocity of Casson fluid is declined with large statistical values of Casson liquid parameter.
- The temperature and concentration are high for enlarge values of Biot number of temperature and concentration.
- The temperature is more with enlarge values of thermal radiation.

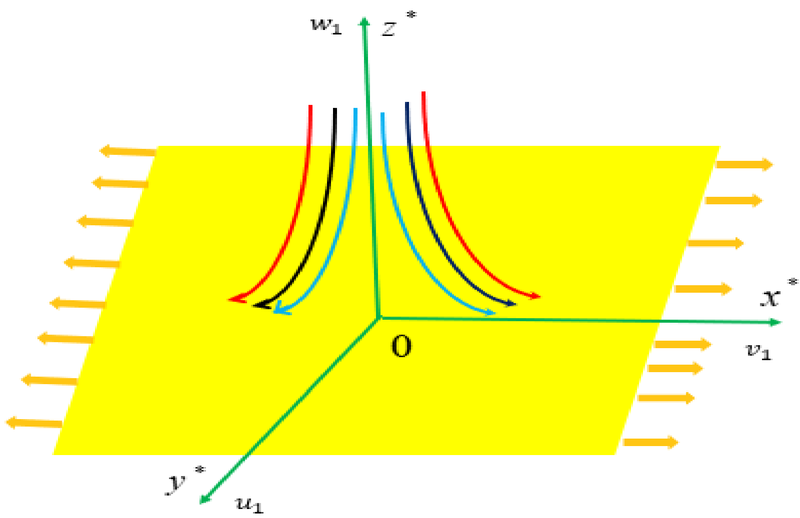

Fig. 1 Physical geometry of the problem

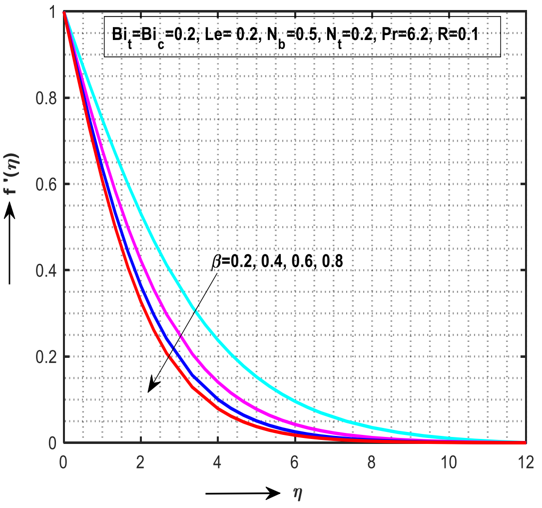

Fig. 2 Influence of β on $f'(\eta)$

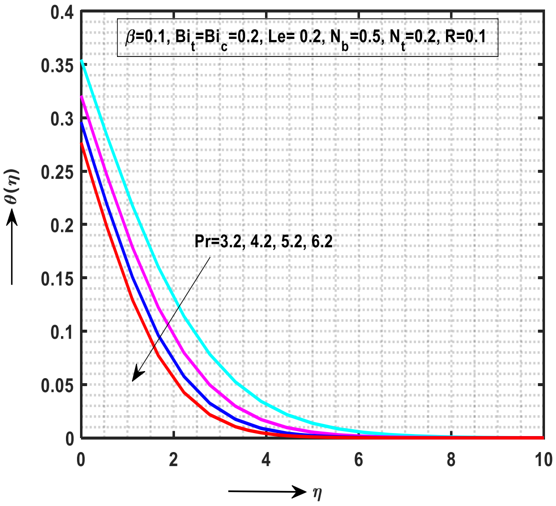

Fig. 3 Influence of Pr on $\theta(\eta)$

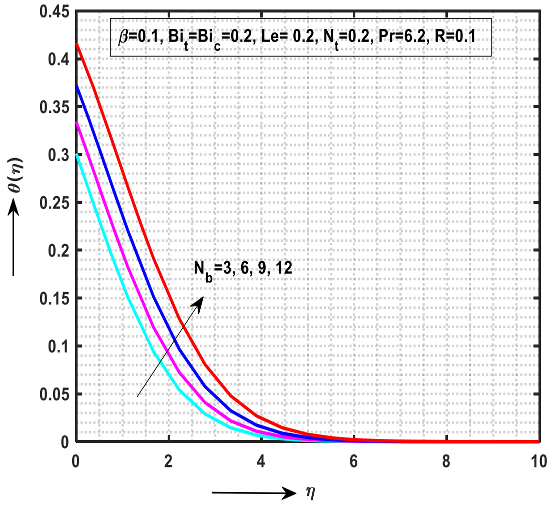

Fig. 3 Influence of N_b on $\theta(\eta)$

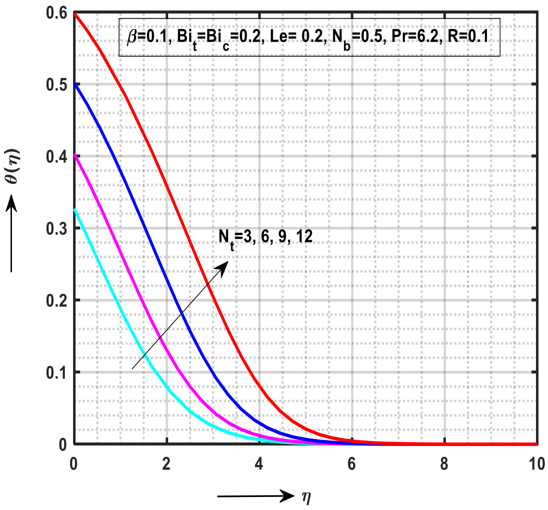

Fig. 4(a) Influence of N_b on $\theta(\eta)$

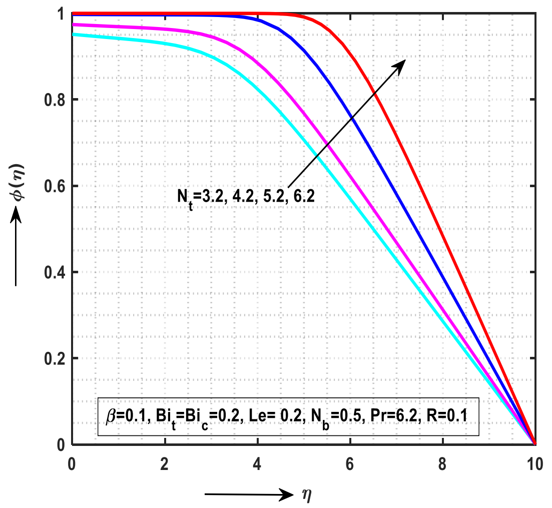

Fig. 4(b) Influence of N_b on $\phi(\eta)$

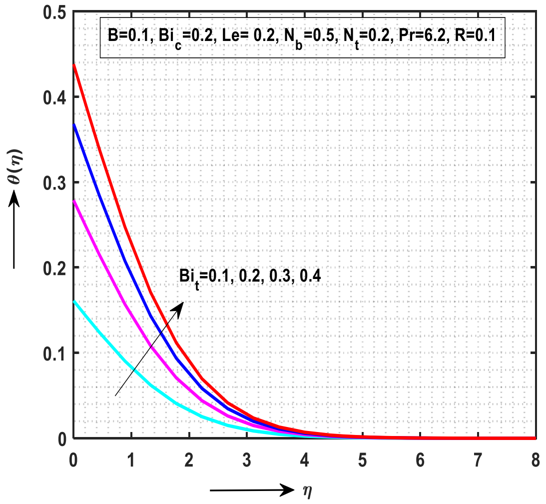

Fig. 5 Influence of Bi_t on $\theta(\eta)$

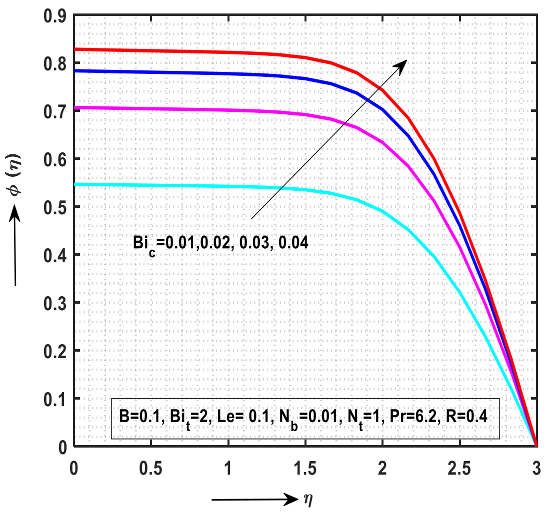

Fig. 6 Influence of Bi_c on $\phi(\eta)$

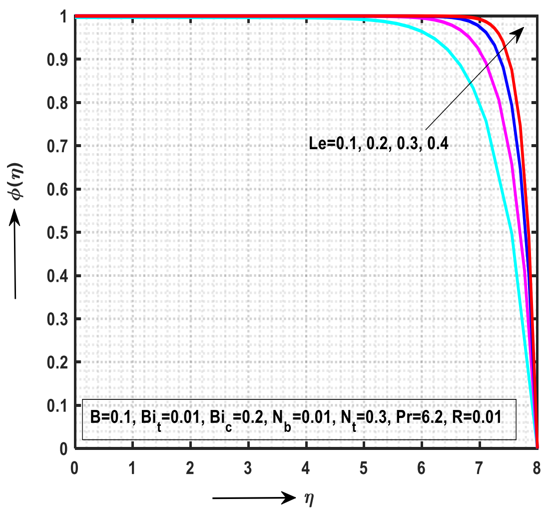

Fig. 7 Influence of Le on $\phi(\eta)$

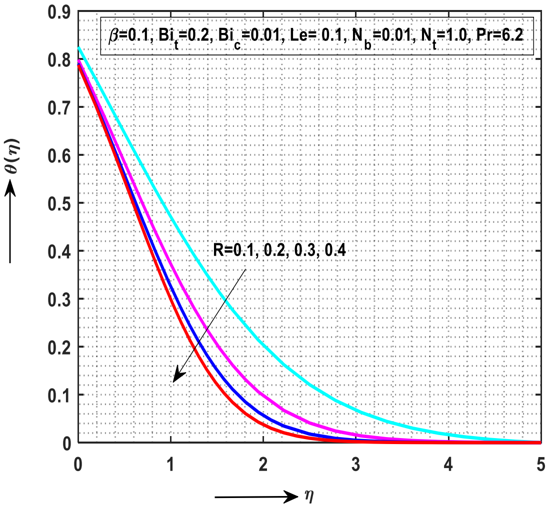

Fig. 8 Influence of R on $\theta(\eta)$

Table 1. Variation of the Casson Fluid Parameter on Skin friction coefficients:

β	$-\left(\frac{1}{1+\beta}\right) f''(\eta)$	$-\left(\frac{1}{1+\beta}\right) g''(\eta)$
∞	1.2105	0.00945
0.5	1.2212	0.12891
1	2.1221	0.32548
1.5	2.2234	0.29358
2	3.0023	0.32546
2.5	3.1589	0.33564
3	3.2558	0.45689
3.5	3.2258	0.44512
4	3.3348	0.45891
4.5	3.4568	0.48901
5	3.5891	0.51254

Table 2. Effect of Brownian motion and Thermophoresis parameter as well as Biot number for temperature and concentration Heat and Mass transfer rate:

N_b	N_t	Bi_t	Bi_c	$-\theta'(0)$	$-\phi'(0)$
0.2	0.1	0.2	0.2	0.52556	0.27456
0.4	0.1	0.2	0.2	0.55652	0.26554
0.6	0.1	0.2	0.2	0.63584	0.28748
0.8	0.1	0.2	0.2	0.44568	0.32221

1.0	0.2	0.2	0.2	0.52556	0.22341
1.2	0.4	0.2	0.2	0.32645	0.22589
1.4	0.6	0.2	0.4	0.52331	0.01245
1.6	0.8	0.2	0.6	0.85472	0.11132
1.8	1.0	0.4	0.2	0.33256	0.44882
2.0	1.2	0.6	0.2	0.52111	0.00200

Refrences

[1] S.U.S. Choi and J.A. Eastman, Enhancing thermal conductivity of fluids with nanoparticles. American Society of Mechanical Engineers, 231 (1995) 99-105.

[2] H. Masuda, A. Ebata, K. Teramea and N. Hishinuma, Altering the thermal conductivity and viscosity of liquid by dispersing ultra-fine particles, Netsu Bussei, 4 (4) (1993) 227-233.

[3] C.Y. Cheng, Natural convection heat transfer of non-Newtonian fluids in porous media from a vertical cone undermixed thermal boundary condition. Int. Comm. Heat Mass Transfer,36 (2009) 693-697.https://doi.org/10.1016/j.icheatmasstransfer .2009.04.006.

[4] E.A.C. Panduro, F. Finotti, G. Largiller and K.Y. Lervåg, A review of the use of nanofluids as heat-transfer fluids in parabolic Trough collectors, Applied Thermal Engineering, 211 (2022) 118346. https://doi.org/10.1016/j.applthermale ng.2022 .118346.

[5] R.M. Mostafizur, M.G. Rasul and M.N. Nabi, Effect of surfactant on stability, thermal conductivity, and viscosity of aluminium oxide – methanol nanofluids for heat transfer applications, Thermal Science and Engineering Progress, 31 (2022) 101302. Https ://doi.org/10.1016/j.tsep .2022.101302.

[6] S. Rangasamy, R.R. Vijaya Raghavan, R.M. Elavarasan and P. Kasinathan, Energy Analysis of Flattened Heat Pipe with Nanofluids for Sustainable Electronic Cooling Applications, Sustainability, *15*(6) (2023) 4716. https://doi.org/10.3390/su15064716

[7] N. Saidulu and A.L. Ventakata, Slip effect on MHD flow of Casson fluid over an exponentially stretching sheet in the presence of thermal radiation, heat source/sink and chemical reaction, Eur. J. Adv. Eng. Tech. (2016) 3 47–55.

[8] A. Khan, Z. Shah, E. Alzahrani and S. Islam, Entropy generation and thermal analysis for rotary motion of hydromagnetic Casson nanofluid past a rotating cylinder with Joule heating effect, International Communications in Heat and Mass Trans, 119 (2020) 104979. https://doi.org/10.1016/j.Icheatmasstrans fer.2020.104979.

[9] A. Zeeshan, O.U. Mehmood, F. Mabood and F. Alzahrani, Numerical analysis of hydromagnetic transport of Casson nanofluid over permeable linearly stretched cylinder with Arrhenius activation energy, International Communications in Heat and Mass Transfer, 130 (2021) 105736. Https://doi.org/10.1016/j.icheatmasstr ansfer .2021.105736.

[10] B. Prabhakar Reddy, O.D. Makinde and A. Hugo, A computational study on diffusion-thermo and rotation effects on heat generated mixed convection flow of MHD Casson fluid past an oscillating porous plate,

International Communications in Heat and Mass Transfer, 138 (2022) 106389. https://doi.org/10.1016/j.icheatmasstransfer.2022.106389.

[11] S. Goud Bejawada, Y. Dharmendar Reddy, W. Jamshed, K. Sooppy Nisar, A.N. Alharbi and R. Chouikh, Radiation effect on MHD Casson fluid flow over an inclined non-linear surface with chemical reaction in a Forchheimer porous medium, Alexandria Engineering Journal, 61(10) (2022) 8207-8220. https://doI.org /10.1016/j.aej.2022.01.043.

[12] M. Riaz Khan, A.S. Al-Johani, A.M.A. Elsiddieg, T. Saeed and A.A. A. Mousa, The computational study of heat transfer and friction drag in an unsteady MHD radiated Casson fluid flow across a stretching/shrinking surface, International Communications in Heat and Mass Transfer, 130 (2022) 105932. https:/doi.org/101016/j. icheatmasstransfer.2021.105832.

[13] P. Jalili, A.A. Azar, B. Jalili and D.D. Ganji, Study of nonlinear radiative heat transfer with magnetic field for non-Newtonian Casson fluid flow in a porous medium, Result in Physics, 48 (2023) 106371.

[14] K. Bhagya Lakshmi, V. Sugunamma, N. Tarakaramu, N. Sivakumar R. Sivajothi, Cross-dispersion effect on magnetohydro dynamic dissipative Casson fluid flow via curved sheet, Heat Transfer, 51(8) (2022) 7822-7842. DOI: 10.1002/htj.22668.

[15] N. Sivakumar, N. Tarakaramu, P.V. Satya Narayan, K. Bhagya Lakshmi and B. Aruna Kumari, Three dimensional magnetohydrodynamic casson fluid flow over a linear stretching surface: A numerical analysis, AIP Conference Proceedings, 2516 (2022) 170022, DOI: 10.1063/5.0110704.

[16] Asifa, P. Kumam, A. Tassaddiq, W. Watthayu, Z. Shah and T. Anwar, Modeling and simulation-based investigation of unsteady MHD radiative flow of rate type fluid; a comparative fractional analysis, Mathematics and Computers in Simulation, 201 (2022) 486-507. https://doi.org/10.1016/j.matcom.2021.02.005.

[17] H. Waqas, U. Farooq, D. Liu, M. Abid, M. Imran and T. Muhammad, Heat transfer analysis of hybrid nanofluid flow with thermal radiation through a stretching sheet: A comparative study, International Communications in Heat and Mass Transfer, 138 (2022) 106303. Https://doi.org/10.1016/j.Icheatmasstra nsfer.2022.106303

[18] M. Yaseen, S. Kumar Rawat, A. Shafiq, Manoj Kumar and K. Nonlaopon, Analysis of Heat Transfer of Mono and Hybrid Nanofluid Flow between Two Parallel Plates in a Darcy Porous Medium with Thermal Radiation and Heat Generation/Absorption, Symmetry, 14(9) (2022) 1943. Https://doi.org/10.3390/sym14091943.

[19] N. Tarakaramu, N. Sivakumar, P.V. Satya Narayana, R. Sivajothi, Viscous Dissipation and Joule Heating Effects on 3D Magnetohydrodynamics Flow of Williamson Nanofluid in a Porous Medium Over a Stretching Surface with Melting Condition, ASME Open Journal of Engineering, 1 (2022) 1-7. DOI: 10.1115/1.4055183.

[20] N. Tarakaramu, P.V. Satya Narayana, R. Sivajothi, K. Bhagya Lakshmi, D. Harish Babu, B. Venkateswarlu, Three-dimensional non-Newtonian couple stress fluid flow over a permeable stretching surface with nonlinear thermal radiation and heat source effects, Heat Transfer, 51(6) (2022) 5348-5367. Doi:10.1002 /htj.22 550.

---

[21] F. Wang, N. Tarakaramu, N. Sivakumar, P.V. Satya Narayana, D. Harish Babu, R. Sivajothi, Three dimensional nanofluid motion with convective boundary condition in presents of nonlinear thermal radiation via stretching sheet, Journal of the Indian Chemical Society, 100(2) (2023) 100887. DOI: 10.1016/j.jics.2023 .100887.

[22] N. Tarakaramu, P.V. Satya Narayana, N. Sivakumar, D. Harish Babu, K. Bhagya Lakshmi, Convective Conditions on 3D Magnetohydrodynamic (MHD) Non-Newtonian Nanofluid Flow with Nonlinear Thermal Radiation and Heat Absorption: A Numerical Analysis, Journal of Nanofluids, 12(2) (2023) 448-457(10). DOI: 10.1166/jo n.2023.1939.

[23] N. Tarakaramu, N. Sivakumar, N. Tamam, P.V. Satya Narayana, R. Sivajothi, Theoretical analysis of Arrhenius activation energy on 3D MHD nanofluid flow with convective boundary condition, Modern Physics Letters B, (2023). DOI: 10.1142/S0217984923410099.

[24] S. Jagadeesh, M. Chenna Krishna Reddy, N. Tarakaramu, H. Ahmad, S. Askar, and S.S. Abdullaev, Convective heat and mass transfer rate on 3D Williamson nanofluid flow via linear stretching sheet with thermal radiation and heat absorption, Scientific Reports, 13 (2023)9889. Https://doi.org/10 .1038 /s41 598-023-36836-4.

[25] S.G. Bejawada and M.M. Nandeppanavar, Effect of thermal radiation on magnetohydrodynamics heat transfer micropolar fluid flow over a vertical moving porous plate, Experimental and Computational Multiphase Flow, 5 (2023) 149-158. Https://doI.org/10 .1007/s42757-021-0131-5.

[26] G.P. Vanitha, U.S. Mahabaleshwar, Z. Liu, X. Yang and B. Sund´en, Magnetohydrodynamic Marangoni boundary layer flow of nanoparticles with thermal radiation and heat transfer in a porous sheet, Case Studies in Thermal Engineering, 44 (2023) 102815. Https://doi.org/10.1016/j.csite.2023.102815.

[27] I.V. Miroshnichenko and M.A. Sheremet, Influence of Thermal Radiation on Heat Transfer through a Hollow Block, Journal of Applied and Computational Mechanics, 9(2) (2023) 419-429. Https://doi.org/10.22055/JACM.2022.41759.3805.

[28] N.I. Ghoneim and A.M. Megahed, Numerical Analysis of the Mixed Flow of a Non-Newtonian Fluid over a Stretching Sheet with Thermal Radiation, Fluid Dynamics & Material Processing, (2023) 1-13. Https://doi.org/10.32604/fdmp .2022 .0205 08.

[29] M. Alrehili, Improvement for engineering applications through a dissipative Carreau nanofluid fluid flow due to a nonlinearly stretching sheet with thermal radiation, Case Studies in Thermal Engineering, 42 (2023) 102768. Https://doi.org/10.1016 /j.csite.2023.102768.

[30] K.U. Rehman, W. Shatanawi and K. Laraib, Mutual impact of thermal radiations and temperature dependent thermal conductivity on non-Newtonian multiple flow regimes, Case Studies in Thermal Engineering, 42(18) (2023) 102752. Https://doI.org/ 10.1016/j.csite.2023.102752.

Nomenclature	
a_1, b_1 Constants	Φ_∞ Ambient fluid temperature
Nu_x Nusselt number	U_∞ Free stream velocity
u_1, v_1, w_1 Velocity components along x^*, y^*, z^*	U_w, V_w Stretching velocities
ψ Nanoparticle volume fraction	W_c Maximum cell swimming speed
ψ_p Specific heat constant $(kJ / kg\ K)$	λ_i Slip factors $= N_i\sqrt{a_1\mu^*}$
ψ_f Skin friction coefficient	***Greek symbols***
ψ_∞ Uniform ambient concentration $(\mathrm{Kg\,m^{-3}})$	ρ_f Fluid density
ψ_w Nanoparticle concentration $(\mathrm{Kg\,m^{-3}})$	$(\rho c)_p$ Heat capacity of the nanoparticle
D_n Diffusivity of microorganisms	$(\rho C)_{bf}$ Base fluid
D_B Brownian diffusion	ρ_f Fluid density
D_T Thermophoresis diffusion $(m^2.\mathrm{s}^{-1})$	$(\rho c)_f$ Heat capacity of the field $(kJ\ kg^{-1})$
f' Dimensionless velocity	ϕ Dimensionless concentration
f Dimensionless stream function	η Similarity variable
h_f Heat transfer coefficient	μ^* Dynamic viscosity $(Pa.\mathrm{s}^{-1})$
k^* Mean absorption coefficient	θ Dimensionless temperature
Le Lewis number $\frac{\alpha_m}{D_B}$	ρ_f Fluid density $(\mathrm{Kg.m^{-3}})$
N_t Thermophoresis parameter $= \frac{\tau^* D_\Phi(\Phi_w - \Phi_\infty)}{\alpha_m \Phi_\infty}$	Bi_t Surface Convection Parameter $\frac{h_f}{k}\left(\sqrt{\upsilon / a}\right)$
N_b Brownian motion coefficient $= \frac{\tau^* D_B(C_w - \psi_\infty)}{\alpha_m}$	Bi_c Surface Convection Parameter $\frac{h_s}{D_B}\left(\sqrt{\upsilon / a}\right)$
N_1, N_2 Slip coefficients in x and y	τ^* Ratio of the nanoparticle to fluid

	$(\rho c)_p / (\rho c)_f$
Pr Prandtl number $= \dfrac{\upsilon^*}{\alpha_m}$	υ^* Kinematic viscosity $= \dfrac{\mu^*}{\rho_f}\left(m^2 s^{-1}\right)$
R Thermal Radiation $= \dfrac{16\sigma^*\Phi_\infty^3}{3k^*K^*}$	***Subscripts***
Φ_f Temperature of hot fluid	∞ condition at free stream
Φ Fluid temperature	w wall mass transfer velocity $(\mathrm{m\,s^{-1}})$
Re_x Reynolds number	
Sc Schmidt number $= \dfrac{\upsilon^*}{D_n}$	
Abbreviations	
HT Heat Transfer	TC Thermal Conductivity
TR Thermal Radiation	NPs Nanoparticles
NFs Nanofluids	SS Stretching Sheet
CF Casson Fluid	